

Simulation of the annual thermal and hydrological cycle in Mexico

V. M. Mendoza, E. E. Villanueva and J. Adem

Centro de Ciencias de la Atmósfera, Universidad Nacional Autónoma de México, México, D. F., México.

Received: September 2, 2001; accepted: February 27, 2002.

RESUMEN

Un modelo no-lineal de balance mensual de agua ha sido desarrollado para estimar el ciclo anual térmico e hidrológico en 12 zonas hidrológicas de México. El modelo incluye la ecuación de balance de energía térmica aplicada a una delgada capa de suelo superficial y la ecuación de balance de agua, usando un déficit de humedad del suelo máximo de 112.5 mm. Estas ecuaciones están acopladas a través de la temperatura del suelo y del déficit de humedad. El modelo tiene cinco parámetros y requiere como datos climáticos la humedad relativa del aire en la superficie, la fracción de cubierta de nubes, la temperatura del aire en la superficie, la velocidad del viento, la precipitación y el albedo de la superficie, así como el flujo de radiación de onda corta sobre la superficie con cielo claro. El modelo proporciona una estimación de la escorrentía superficial y sub-superficial, la humedad del suelo, la radiación neta, los flujos de calor sensible y calor latente, la temperatura del suelo y el índice de aridez. El mapa de escorrentía anual total (superficial más sub-superficial) calculado por el modelo muestra un notable parecido con el correspondiente mapa de valores observados. La escorrentía mensual total (superficial más sub-superficial) calculada por el modelo muestra una variación mensual similar a la observada en los ríos de cada zona hidrológica. El conjunto de mapas observados de temperatura del suelo y disponibilidad de humedad del suelo calculados para enero y julio por el modelo son comparados con los correspondientes mapas obtenidos de los reanálisis del Centro Nacional para Predicción del Medio Ambiente (NCEP); las comparaciones muestran ciertas similitudes entre ambos conjuntos de mapas; sin embargo, en ciertas regiones existen notables diferencias en estas dos variables.

PALABRAS CLAVE: Ciclo térmico e hidrológico, flujo de calor y agua, disponibilidad de la humedad del suelo, temperatura del suelo superficial.

ABSTRACT

A nonlinear monthly water balance model for twelve hydrologic zones of Mexico is presented. The balance thermal energy equation applied to a thin soil surface layer and the water balance equation with maximum soil moisture deficit of 112.5 mm are coupled through the soil temperature and the soil moisture deficit. The model has five parameters. Input data are surface air relative humidity, cloudiness, surface air temperature, surface wind speed, precipitation, surface albedo, and the short wave radiation at the surface with clear sky. The model gives an estimate of the monthly surface and subsurface runoff, the soil moisture, the net radiation, the sensible and latent heat, the soil temperature and the annual dryness index. The computed total annual runoff (surface plus subsurface) agrees with the map of observed values. The computed monthly total runoff values show monthly variations similar to those observed in rivers of each hydrological zone. The maps of soil surface temperature and moisture availability computed for January and July show some similarities with the maps from the National Center for Environmental Prediction large-scale reanalysis.

KEY WORDS: Thermal and hydrological cycle, heat and water flux, soil moisture availability, soil surface temperature.

1. INTRODUCTION

Climate and hydrology are strongly linked at local, regional and global scales. In Mexico the influence of climate change on the hydrological cycle is complex. Modeling the physical processes governing the interaction between climate and hydrology can improve the understanding of the balance between precipitation, evapotranspiration, runoff and change in water storage. According to Schaake (1990), as a first approximation, a linear water balance model may be used to estimate how precipitation and potential evapotrans-

piration affect runoff. However, a linear model does not yield a good estimate of the runoff in semiarid basins. In northern Mexico (22 to 32 degrees latitude North) the basins are semiarid, while in the south (10 to 22 degrees latitude North) they are humid. Thus a linear model is not adequate for modeling the runoff in the northern basins of Mexico.

Schaake (1990) developed a nonlinear monthly water balance model of five parameters that may be applied in semiarid and humid basins. This model was calibrated for the Oklahoma and China river basins, as well as the southeast-

ern contiguous United States, to simulate the runoff in 52 river basins.

The first version of this non-linear water balance model was applied to the study of the vulnerability of basins and watersheds in Mexico to global climate change (Mendoza *et al.*, 1997). In this work we show a new version of the model to estimate the annual thermal and hydrologic cycle in twelve hydrological zones in which is Mexico divided. To compute the soil temperature, we use the thermal energy balance equation with a similar method to the one used by Ohta *et al.* (1993). In addition, this equation is coupled with a nonlinear monthly water balance equation similar to the one proposed by Schaake (1990).

2. MODEL DESCRIPTION

The main equations in the nonlinear monthly water balance model are the thermal energy balance equation applied to a thin soil surface layer and the water balance equation. These equations are coupled through the soil surface temperature and the soil moisture deficit.

The monthly soil surface temperature is determined by the thermal energy balance equation:

$$0 = E_s - G_2 - G_3 - G_s, \quad (1)$$

where E_s is the net radiation; G_2 , the sensible heat flux given off to the atmosphere by vertical turbulent transport; G_3 , the latent heat flux at the soil surface and G_s , the sensible heat flux conducted in or out of the thin surface layer.

The monthly change in the soil moisture deficit is computed from the water balance equation, neglecting the transfer of groundwater across basin boundaries (Schaake, 1990):

$$\frac{\partial D}{\partial t} = E + Q - P, \quad (2)$$

where D is the soil moisture deficit variable, E is the evapotranspiration at the soil surface, Q is the runoff and P is the precipitation.

2.1. Parameterizations of heat and water fluxes.

The net radiation at the soil surface (in Wm^{-2}), applicable for climatological averages of the variables, is computed using the formula given by Budyko (1974):

$$E_s = -\delta\sigma T_a^4 \left[0.254 - 0.00495 U_a e_s(T_a) \right] (1 - c\varepsilon) - 4\delta\sigma T_a^3 (T_s - T_a) + \alpha_1 I, \quad (3)$$

where T_s is the soil surface temperature (in K), $\delta = 0.96$ is the emissivity of the soil, $\sigma = 5.67 \times 10^{-8} Wm^{-2}K^{-4}$ is the Stefan-Boltzmann constant, T_a (in K) and U_a (in fractions of unity), the air temperature and the air relative humidity respectively, at some level Z_a (in m) above the soil surface; $e_s(T_a)$ is the saturation vapor pressure in hPa at the air temperature, ε is the fractional amount of cloudiness, $c = 0.65$ is a cloud cover coefficient and $\alpha_1 I$ is the short wave radiation (in Wm^{-2}) absorbed by the soil surface layer.

For $\alpha_1 I$ we use the Berliand-Budyko formula:

$$\alpha_1 I = R_0 [1 - (a + b\varepsilon)\varepsilon] (1 - \alpha_s), \quad (4)$$

where R_0 is the total radiation received by the soil surface with clear sky (in Wm^{-2}), $a = 0.35$ and $b = 0.38$ are constants which were taken from Budyko (1974), and α_s is the albedo of the soil surface (in fractions of unity).

For the sensible heat flux (in Wm^{-2}), we use the following formula:

$$G_2 = \frac{\rho_a c_p}{r_a} (T_s - T_a), \quad (5)$$

where r_a is the aerodynamic resistance to the sensible heat flux in sm^{-1} ; $\rho_a = 1.225 kg m^{-3}$ is the surface air density; $c_p = 1.004 J kg^{-1}K^{-1}$, the specific heat of the air at constant pressure.

The value of r_a was computed, following Famiglietti and Wood (1994), with the formula:

$$r_a = \frac{1}{k^2 |V_a|} \left[\ln \left(\frac{Z_a - d}{Z_0} \right) \right]^2, \quad (6)$$

where $k = 0.41$ is von Kármán's constant, $|V_a|$ is the wind speed in ms^{-1} at the level $Z_a > Z_0 + d$, d is the zero plain displacement and Z_0 is the roughness length of the soil surface, both in meters. The Z_0 value for each of the hydrological zones of Mexico were taking from Benjamin and Carlson (1986), and the corresponding values of d from Oke (1987).

Following Oke (1987), the sensible heat flux into the ground (in Wm^{-2}) is given by:

$$G_s = -\Lambda (T_s - T_1), \quad (7)$$

where $\Lambda = \lambda \sqrt{\frac{\pi}{\kappa\tau}}$ is the apparent conductivity (in $Wm^{-2}K^{-1}$) of the ground layer; T_1 is the temperature at depth z_1 , which is equal to λ / Λ ; λ is the thermal conductivity (in $Wm^{-1}K^{-1}$),

which depends upon the conductivity of the soil particles, the soil porosity and the soil moisture; τ is the period (s) of the soil temperature variation, which is wave-like, and κ is the thermal diffusivity of the soil (m^2s^{-1}). Typical values of κ and λ for a non-saturated soil clay are $0.40 \times 10^{-6} m^2s^{-1}$ and $1.0 Wm^{-1}K^{-1}$, respectively. For an annual period $\tau = 3.15 \times 10^7 s$, $\Lambda = 0.5 Wm^{-2}K^{-1}$ and $z_1 = 2m$. From generalized cycles of soil temperature at different depths for an annual period given by Oke (1987), we have estimated that a maximum value of $T_s - T_1$ is 7 K in July, therefore $3.5 Wm^{-2}$ is a maximum value representative for G_s . For the net radiation E_s , Jauregui (1978) has estimated, for the central part of Mexico, values of 100 and $137 Wm^{-2}$ for January and July, respectively. Therefore, this result shows that, on the basis of the above approach, for an annual period the sensible heat flux into the ground in equation (1) is neglected and that the net radiation is balanced mainly by the sensible and latent heat fluxes.

For the latent heat flux (in Wm^{-2}), we use the following formula:

$$G_3 = \rho_w LE, \quad (8)$$

where $\rho_w = 1.0 \times 10^3 kg m^{-3}$ is the water's density and $L = 2.45 \times 10^6 J kg^{-1}$ is the latent heat of vaporization of water and E is the evapotranspiration.

We assumed that the monthly evapotranspiration E is a fraction of the rate of evaporation from a free water surface (called potential evapotranspiration E_p) whose temperature is equal to the soil surface temperature, that is:

$$E = \left(\frac{D_{max} - D}{D_{max}} \right) E_p, \quad (9)$$

where D_{max} is the maximum value of D . The evaporation E in any month is a fraction of E_p decreasing from 1 when D is zero until zero when $D = D_{max}$. If D is zero the storage system is saturated to its limit. The term $(D_{max}-D)/D_{max}$ in equation (9) is called the *moisture availability*.

The potential evapotranspiration is computed applying the thermal energy balance equation (1) to free water surface taking $G_s = 0$, assuming that the aerodynamic resistance in the sensible heat and in the latent heat are equal, and using the following approximation:

$$e_s(T_s) = e_s(T_a) + \Delta(T_s - T_a),$$

where $e_s(T_s)$ is the saturation vapor pressure in hPa at the soil surface temperature and Δ is the slope of the curve of e_s to the air temperature. Therefore, we obtain the following equa-

tion for E_p as a function of the net radiation E_s at the free water surface, and the vapor pressure deficit, $e_s(T_a) - U_a e_s(T_a)$:

$$E_p = \frac{1}{\rho_w L} \left\{ \frac{\Delta E_s + \rho_a C_p (e_s(T_a) - U_a e_s(T_a)) / r_a}{\Delta + \gamma} \right\}, \quad (10)$$

where r_a is the aerodynamic resistance exerted by the air near the free water surface, which is computed from formula (6) taking $Z_a = 2m$, $d = 0$ and $Z_0 = 1.0 \times 10^{-4} m$ (Oke, 1978), and γ is the psychrometric constant. In formula (10), the net radiation E_s is computed by Equation (3), assuming that the surface longwave emissivity for water is equal to that of its soil, and using the albedo of the free water surface taken as 0.08 in Equation (4). Equation (10) is similar to the so-called Penman-Monteith equation for the case in which the canopy resistance is equal to zero.

The runoff (in $mm day^{-1}$) is the sum of the surface runoff Q_s and the subsurface runoff Q_g :

$$Q = Q_s + Q_g. \quad (11)$$

The surface runoff is computed using a similar equation to the one used in the Soil Conservation Service curve number method (SCS, 1960):

$$Q_s = \left(\frac{P_X}{P_X + D} \right) P_X, \quad (12)$$

where P_X is the precipitation (in $mm day^{-1}$) contributing to the surface runoff, which according with Schaake (1990) is given by:

$$P_X = P - \Theta E - zD, \quad (13)$$

where $\Theta \leq 1$ is the proportion of E that must be satisfied from P (mm) in the current month before storm runoff or infiltration can occur and $z \leq 1$ is the proportion of D that must be satisfied by infiltration before any storm runoff. If P_X is positive, then storm runoff can occur.

The subsurface runoff is assumed to vary with the deficit D according with the following expression:

$$Q_g = Q_{gmax} \left(1 - \frac{D}{S_{max}} \right), \quad (14)$$

where Q_{gmax} (in $mm day^{-1}$) is the maximum values of Q_g when the storage system is saturated to its limit ($D = 0$) and S_{max} (in mm) is a parameter, such that the constant rate Q_{gmax} / S_{max} is a measurement of how fast water flows from groundwater to streams. If D exceeds S_{max} , Q_g is zero.

2.2. The integration method

Equations (1) and (2) are applied to time-average variables of one month, and for their integration we shall apply an implicit scheme in 106 points distributed over twelve hydrological zones in Mexico, which are shown in Figure 1, and that we have obtained from the 37 official Mexican hydrological regions (Atlas del Agua, 1976) following similar hydrological characteristics.

The soil surface temperature is computed from Equation (1) assuming that the sensible heat flux conducted into the ground is neglected and considered that the net radiation E_s , the sensible heat flux G_2 , and the latent heat flux G_3 , given by (3), (5) and (8), respectively, can be expressed by:

$$\begin{aligned} E_s &= E_1^* + E_2^*(T_s - T_a) \\ G_2 &= E_3^*(T_s - T_a) \\ G_3 &= E_6^* + E_7^*(T_s - T_a), \end{aligned} \quad (15)$$

where

$$\begin{aligned} E_1^* &= -\delta \sigma T_a^4 [0.254 - 0.0066 U_a e_s(T_a)](1 - c\varepsilon) + \alpha_1 I \\ E_2^* &= -4\delta \sigma T_a^3 \\ E_3^* &= \rho_a c_p C_H |V_a| \end{aligned}$$

$$\begin{aligned} E_4^* &= \left(\frac{\rho_a c_p}{\gamma} \right) \frac{[1 - U_a]}{r_a} e_s(T_a) \\ E_6^* &= \left(\frac{D_{max} - D}{D} \right) \left[\frac{\Delta}{\Delta + \gamma} E_{1w}^* + \frac{\gamma}{\Delta + \gamma} E_4^* \right] \\ E_7^* &= \left(\frac{D_{max} - D}{D} \right) \frac{\Delta}{\Delta + \gamma} E_2^* \end{aligned} \quad (16)$$

and where E_{1w}^* is computed as E_1^* but using, in $\alpha_1 I$, the albedo of water surface which is given by Equation (4).

Using (15), Equation (1) becomes linear algebraic in T_s , therefore we get:

$$T_s = T_a + \frac{E_6^* - E_1^*}{E_2^* - E_3^* - E_7^*}. \quad (17)$$

According with the last two expressions in (16), the soil temperature given by (17) is a function of the soil moisture deficit variable.

The term $\partial D / \partial t$, in Equation (2) is replaced by $(D - D_p) / \Delta t$, with $\Delta t = 30$ days, where D_p is the value of D in the previous month, both give in mm; in this case, the runoff (Q) and the precipitation (P) are given in mm day⁻¹, and the fac-

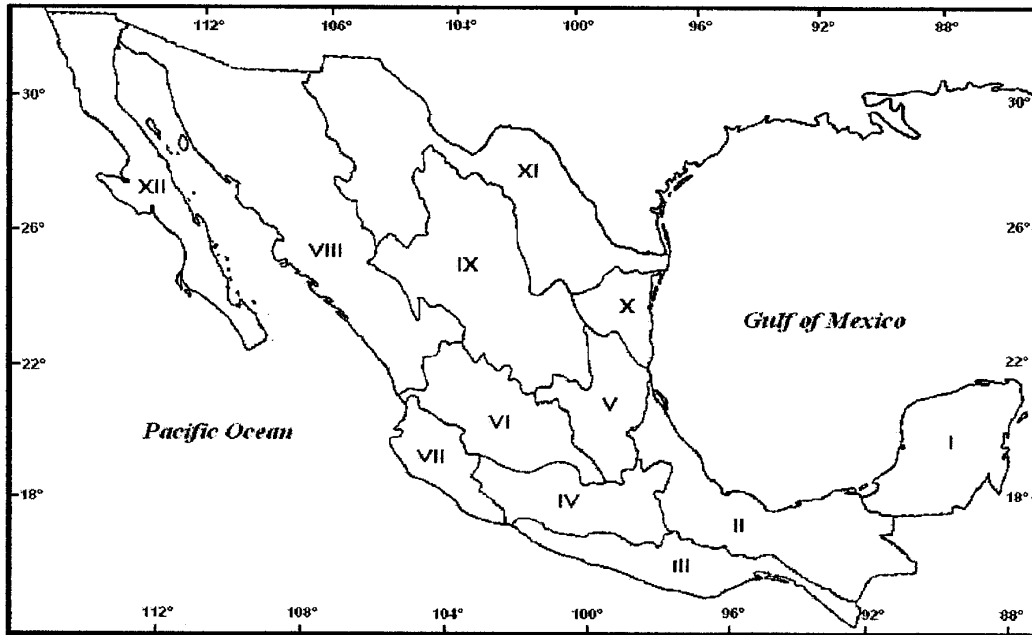


Fig. 1. The 12 hydrological zones into which the Mexican territory was divided. (I) Campeche-Yucatán-Quintana Roo plains, (II) Southern Gulf Watershed, (III) Southern Pacific Watershed, (IV) Balsas River Basin, (V) Pánuco River Basin, (VI) Lerma-Chapala-Santiago Basin, (VII) Central Pacific Watershed, (VIII) Northern Pacific Watershed, (IX) Mapimi-Aguanaval- El Salado Closed Basin, (X) Northern Gulf Watershed, (XI) Rio Bravo and Northern Closed Basin, and (XII) Baja California Peninsula.

tor $1 / \rho_w L$ in (10) is multiplied by 0.864×10^8 to obtain the potential evapotranspiration (E_p) and the evapotranspiration (E), given by (9), in mm day^{-1} . Therefore, Equation (2) can be expressed as:

$$D = D_p + \Delta t(E + Q - P) . \quad (18)$$

In Equation (18), the evaporation E and the runoff Q are functions of the moisture deficit variable D and of the potential evaporation E_p . Therefore, substituting the soil temperature T_s given by (17), in Formula (10), the problem is reduced to solving the non-linear Equation (18) for the moisture deficit variable D .

To generate the annual soil surface temperature and the soil moisture deficit variable, as well as the heat and the water fluxes for each point over the twelve hydrological zones in Mexico, Equation (18) is solved by the Newton's method (Carnahan *et al.*, 1969), using the following seven observed climate variables T_a , U_a , $|V_a|$, ϵ and P , obtained from the Atlas del Agua de la República Mexicana (1976); R_0 , obtained from the files of the Adem thermodynamic climate model (Adem, 1964) and values of α_s for dry and wet soil surface, obtained from Barradas (1990).

The atmospheric surface conditions, the cloudiness, the precipitation, the total short wave radiation and the surface albedo are prescribed month to month, so that they change after one time-step. We start the computations with an initial uniform soil temperature of 20°C and soil moisture deficit of D_{\max} in the whole integration region. Starting in January, the integration was carried out for 10 years until the computed average values of soil temperature and soil moisture deficit, for each of the 12 months of the year, had a difference of less than 0.001°C and 0.001 mm with the corresponding values of the previous year.

The annual values of evapotranspiration and total runoff should satisfy the following annual water balance equation:

$$0 = E_A + Q_A - P_A, \quad (19)$$

where the subscript A means annual values.

3. RESULTS

The model has five hydrological parameters: D_{\max} , S_{\max} , G_{\max} , Θ , and z . Schaake (1996) has suggested that usually $S_{\max} < D_{\max}$. In this work, we use $D_{\max} = 112.5 \text{ mm}$ for all zones, this value is the 75% of the field capacity of the soil moisture layer of 150 mm of water as was chosen by Manabe (1969).

The method of SCS assumes in Equation (13) only initial loss by infiltration which is equal to 20% of the infiltration capacity ($z = 0.2$). According with Bá *et al.*, (1995), the experience shows that the value $z = 0.2$ obtained by the SCS-method is very high, even for humid basins. Springer *et al.* (1980) found that z is lower than 0.20 for humid and semi-arid basins. Fogel *et al.* (1980) used $z = 0.15$. In this work we assume $z = 0.10$ for all zones.

We added to the initial loss by infiltration, a 10% of initial loss by evapotranspiration for all zones, that is, $\Theta = 0.10$. According to Schaake (personal communication), this value is reasonable for the proportion of E that must be satisfied from the precipitation in the current month before storm runoff or infiltration can occur.

The parameter G_{\max} is computed using the relation $G_{\max}/S_{\max} = 0.028$ for all zones. This value is an average of the different values found by Schaake (1996) for the Bird Creek Basin (USA).

The remaining parameter S_{\max} is adjusted until the value of the annual runoff for all the country computed by the model agree well enough with the corresponding observed value of 208.3 mm . We found that $S_{\max} = 64.2 \text{ mm}$ and therefore $G_{\max} = 1.798 \text{ mm}$ for all the country.

Table 1 shows the area of each zone and of all the country, the annual precipitation and the annual runoff (in mm) estimates from observed data of the Atlas del Agua de la República Mexicana (1976), as well as the annual evapotranspiration obtained from the annual water balance Equation (19).

Figure 2 shows the annual runoff (surface plus subsurface runoff) simulated by the model (Figure 2A) and observed (Figure 2B) for the arid and semi-arid basins, in a scale of 1 to 10 cm. Figure 3 is similar to Figure 2, but for humid basins in a scale of 10 to 100 cm. The comparison of Figure 2A with Figure 2B and Figure 3A with Figure 3B shows good agreement between the simulated and the observed annual runoff.

Observed and simulated annual runoff for each of the 12 hydrologic zones are compared in Figure 4. In a similar way than Schaake (1996), the errors of 50% are shown on either side of the line of equal observed and simulated values; 9 zones lie inside these limits. The zones I, VII and X with errors of 57.0%, 137.1% and 121.3%, respectively, lie outside these limits.

Figure 5 is similar to Figure 4 but for the evapotranspiration; in this case we have considered the errors found of 20%. All the zones lie inside these limits.

Table 1

Area in km^2 (second column), observed annual precipitation in mm (third column), observed annual runoff in mm (fourth column) and annual evapotranspiration, computed from Equation (19), for each hydrological zone of Mexico and for the whole country, obtained from Atlas del Agua de la República Mexicana (1976)

<i>Hydrological Zone</i>	<i>Area in km^2</i>	<i>Annual Precipitation mm.</i>	<i>Annual Runoff in mm</i>	<i>Annual Evaporation mm</i>
I	139626	1247.0	213.8	1033.2
II	197803	1863.7	945.5	918.2
III	90774	1447.2	724.0	723.2
IV	116912	1064.6	248.1	816.5
V	95682	756.9	220.2	536.7
VI	130428	761.1	79.6	681.5
VII	57263	1099.4	366.6	732.8
VIII	361455	515.8	95.3	420.5
IX	252927	365.0	11.9	353.1
X	51962	739.3	40.6	698.7
XI	329927	447.9	18.6	429.3
XII	143789	146.5	2.0	144.5
Country	1967948	772.0	208.3	563.7

Table 2 shows in mm the computed annual values of: total runoff Q , subsurface runoff Q_s , evapotranspiration E and potential evapotranspiration E_p , as well as the ratios E/P , Q/P , Q_s/Q and P/E_p for each hydrological zone and for the whole country. The annual precipitation over Mexico is 772.0 mm (Table 1), the annual runoff to the oceans, computed or observed (Table 1 or Table 2), is 208.3 mm ($410,021 \times 10^6 m^3$), according with the water balance Equation (19), the difference between these values is the average annual evapotranspiration which is equal to 563.7 mm, and which represents the 73% of the precipitation.

Table 2 shows that in each hydrological zone, the sum of the annual runoff and the annual evaporation is equal to the observed annual precipitation shown in Table 1, indicating that the model satisfies the annual water balance Equation (19).

According with Table 2, the subsurface runoff is an important fraction of the total runoff, in the zones I, IV, V, VI, VIII, X and XI is larger than half of the total runoff, and in the zones IX and XII is the 100% of the total runoff.

The last column of Table 2 shows the ratio P/E_p , which can be considered as a drought index of the zone, according

to the World Meteorological Organization. Zones with an index higher than 0.50 can be considered as wet zones, zones with an index smaller than 0.50 but larger than 0.20 are considered semi-wet zones and zones with an index equal or smaller than 0.20 are considered as arid zones. The zones II and III, with indices of 1.06 and 0.81 respectively, are the wettest zones of the country. The zone XII has an extreme aridity, since $P/E_p = 0.1$.

Monthly percentages relative to the annual value of the observed precipitation, simulated subsurface runoff and total runoff, as well as the observed river runoff in the hydrological zones II and III (Figure 6), show that the subsurface runoff is practically zero during dry spell (low-water months) for the zone II and zero for the zone III, in disagreement with the observed river runoff. In the rainfall months the total runoff is like the precipitation regime. In these zones, considered as examples, there is certain similarity between simulated and observed total runoff.

Figure 7 shows the soil surface temperatures simulated by the model (Part A) and the skin temperature obtained from large-scale NCEP reanalysis (Part B) for January, in Celsius degree. Figure 8 is similar to Figure 7 but for July. From the comparison of Part A and Part B of Figures 7 and 8, we find

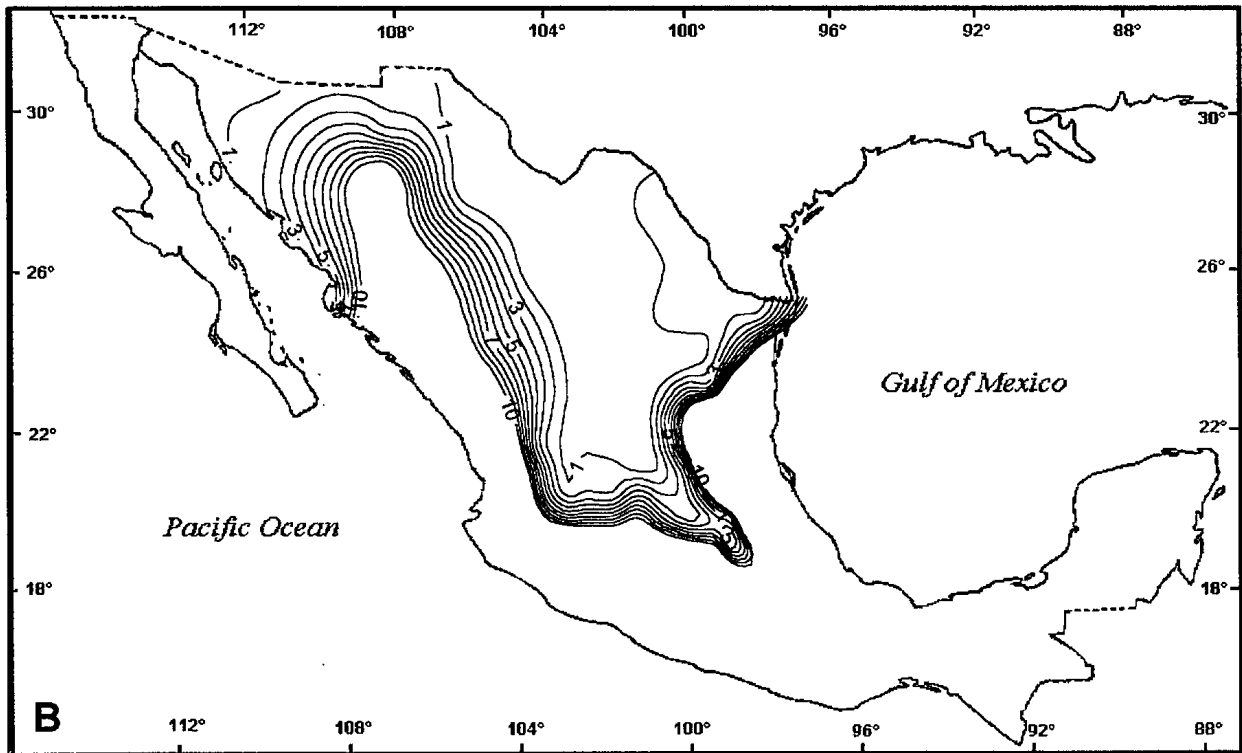
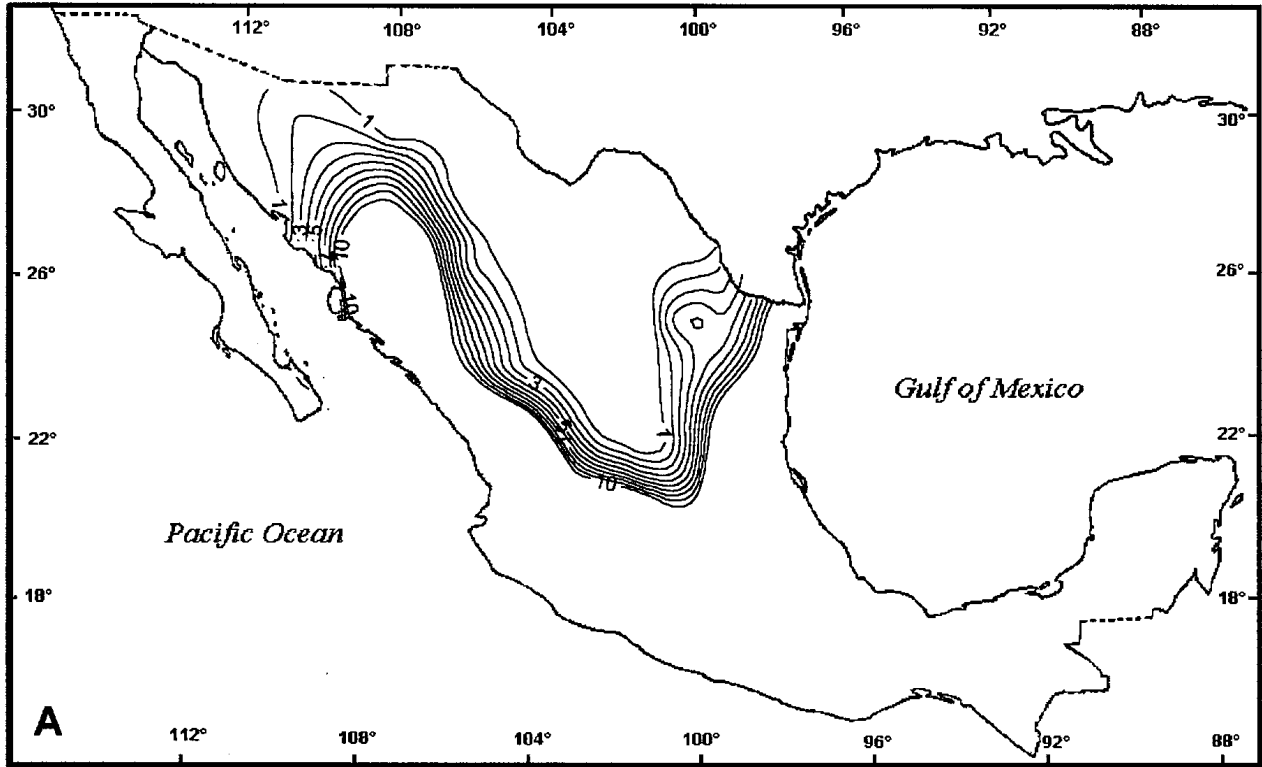


Fig. 2. Annual runoff (surface plus subsurface runoff) simulated by the model (Part A) and observed (Part B) for arid and semi-arid regions, on a scale of 1 to 10 cm.

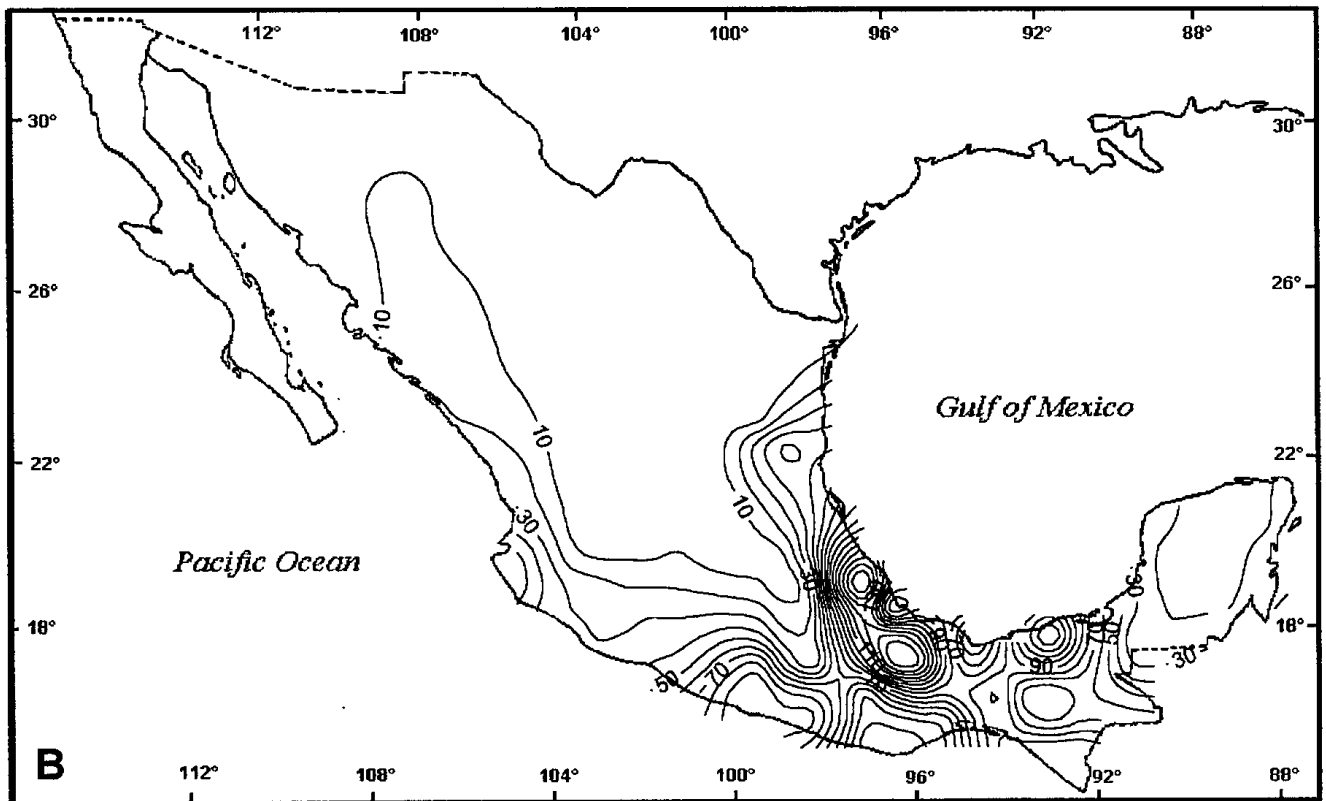
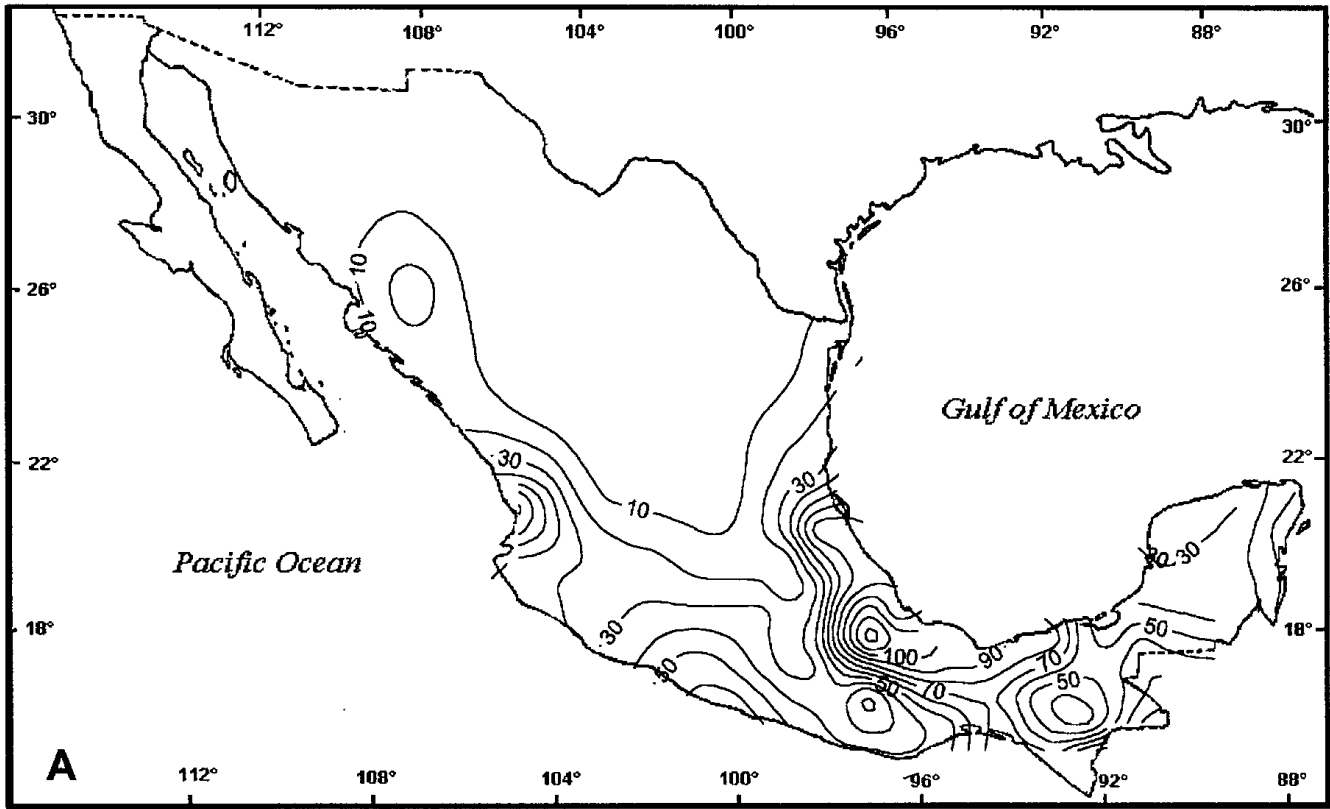


Fig. 3. Similar to Figure 2 but humid regions, on a scale of 10 to 100 cm.

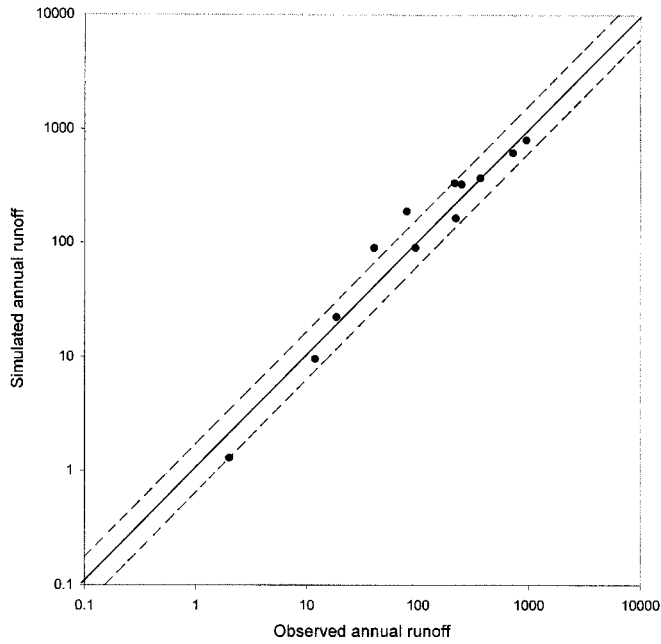


Fig. 4. Observed vs. simulated annual runoff for each 12 hydrological zones. The errors of 50% are shown on either side of the line of equal observed and simulated values.

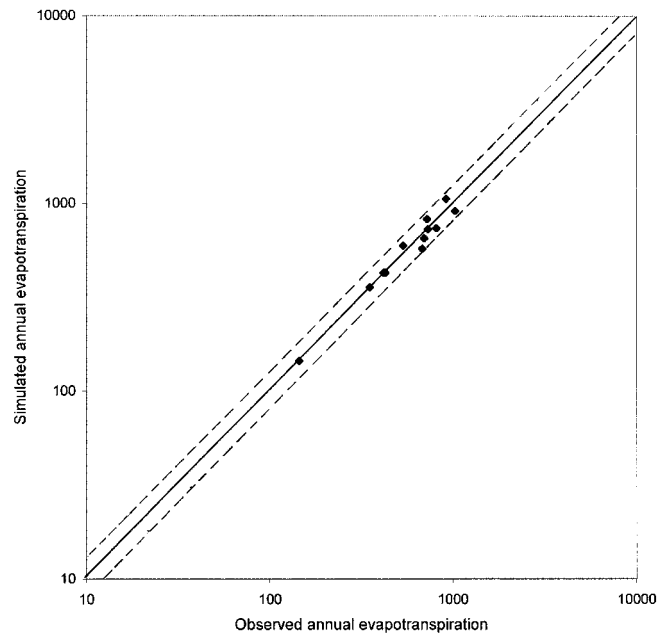


Fig. 5. Observed vs. simulated annual evapotranspiration for each 12 hydrological zones. The errors of 20% are shown on either side of the line of equal observed and simulated values.

Table 2

Computed annual values, in mm, of total runoff Q , ground water runoff Q_g , evapotranspiration E and potential evapotranspiration E_p , as well as the ratios E/P , Q/P , Q_g/Q and P/E_p for each hydrological zone and for the whole country

<i>Zone</i>	Q	Q_g	E	E_p	E/P	Q/P	Q_g/Q	P/E_p
I	335.7	213.2	911.4	1616.0	0.73	0.27	0.64	0.78
II	805.1	274.9	1058.6	1774.3	0.57	0.43	0.34	1.06
III	622.3	211.5	824.8	1846.5	0.57	0.43	0.34	0.81
IV	327.9	170.5	736.7	1779.8	0.69	0.31	0.52	0.60
V	164.0	117.8	592.9	1368.2	0.78	0.22	0.72	0.56
VI	188.7	132.0	572.4	1494.6	0.75	0.25	0.70	0.51
VII	372.3	158.6	727.1	1930.8	0.66	0.34	0.43	0.58
VIII	90.5	54.2	425.2	1658.7	0.82	0.18	0.60	0.33
IX	9.6	9.6	355.4	1615.3	0.97	0.03	1.00	0.23
X	89.9	64.1	649.4	1758.0	0.88	0.12	0.71	0.42
XI	22.3	18.1	425.6	1795.4	0.95	0.05	0.81	0.26
XII	1.3	1.3	145.2	1615.5	0.99	0.01	1.00	0.10
Country	208.3	97.7	563.7	1683.4	0.73	0.27	0.47	0.46

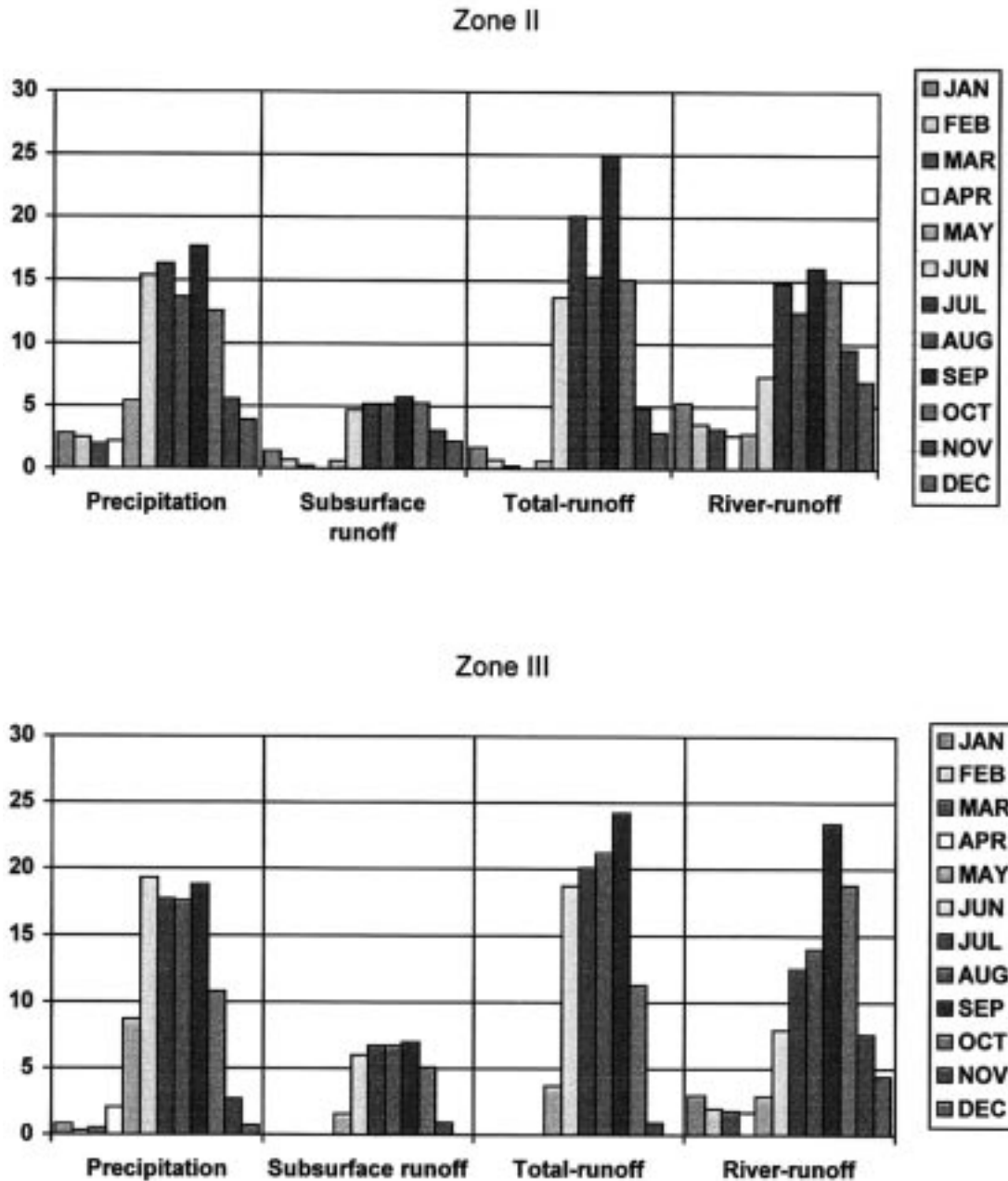


Fig. 6. Montly percentage relative to the annual value of the observed precipitation, simulated subsurface runoff and total runoff, as well as the observed river runoff, the upper part corresponding to zone II and the lower part to zone III.

that except in the northwest part of Mexico, where the soil surface temperature is significantly greater than the skin temperature (4 degrees in January and 10 degrees in July). In the rest of the country the values of the soil surface temperature and of the skin temperature are very similar indicating that the model has some skill to simulate this variable.

Figure 9 shows the soil moisture availability, simulated by the model (Part A) and the quotient of the latent heat over the potential evaporation (Part B), both obtained from the

NCEP reanalysis for January. Figure 10 is similar to Figure 9 but for the case of July. The intensive rain of the Mexican monsoon in July produces an increase in the soil moisture availability simulated by the model in the northwest region (Figure 10, Part A), but the corresponding map from the NCEP reanalysis (Figure 10, Part B) does not show this increase.

According to Equation (17), the soil surface temperature is expressed as the surface air temperature plus a correc-

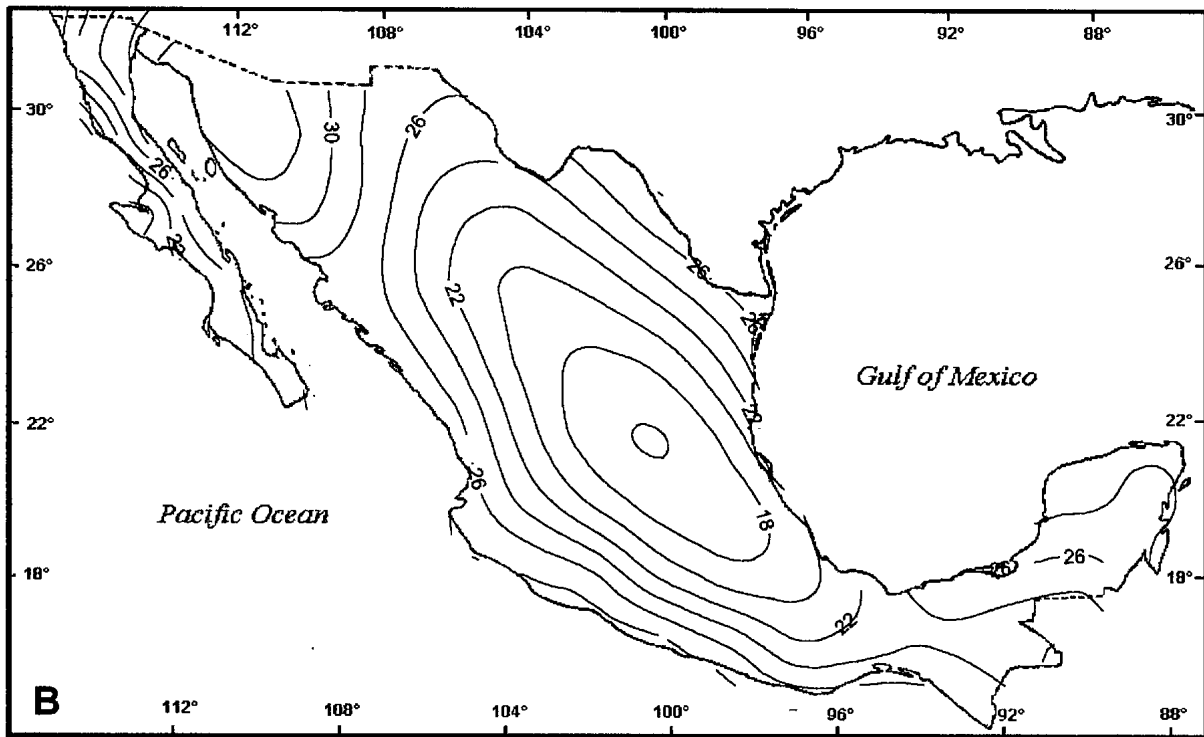
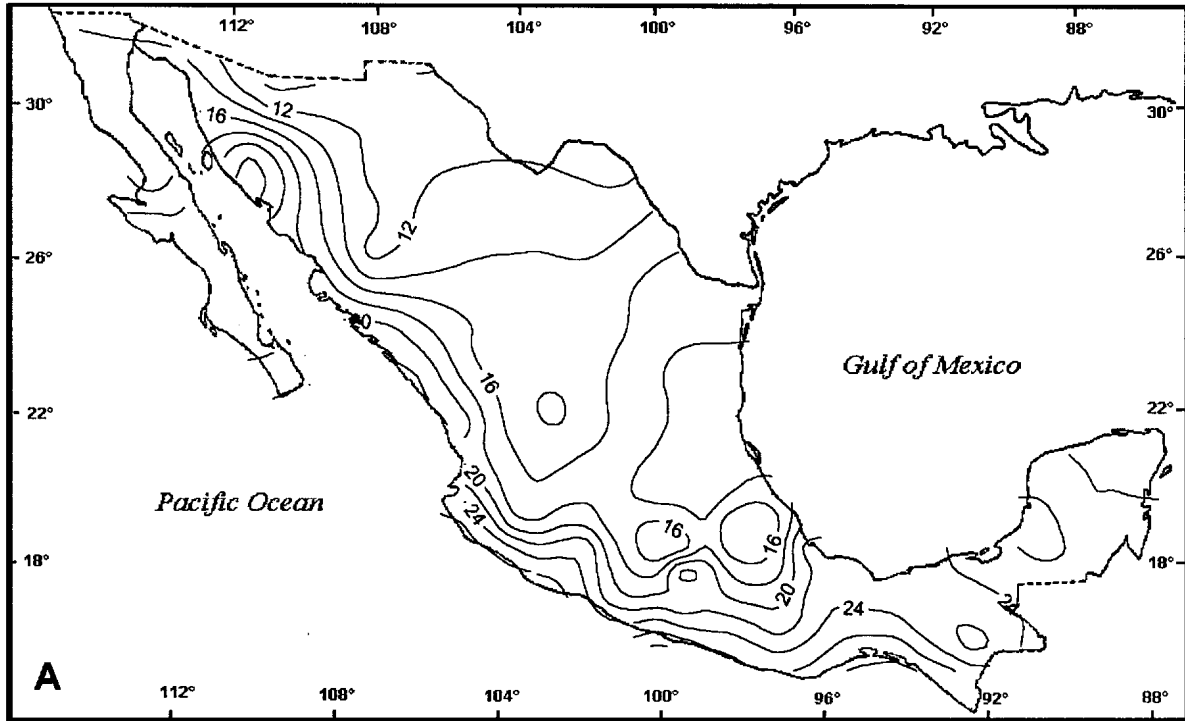


Fig. 7. Soil surface temperature for January, in Celsius degree, simulated by the model (Part A) and the skin temperature obtained from large-scale NCEP reanalysis (Part B).

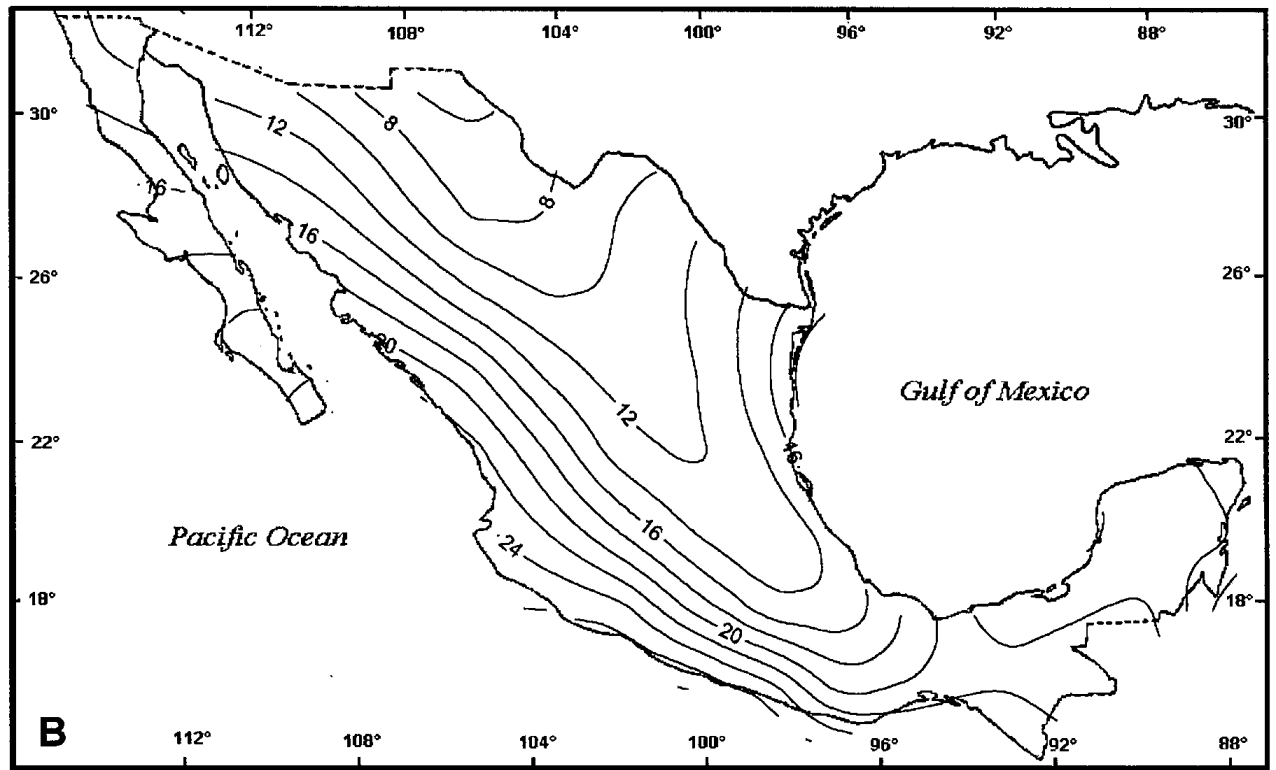
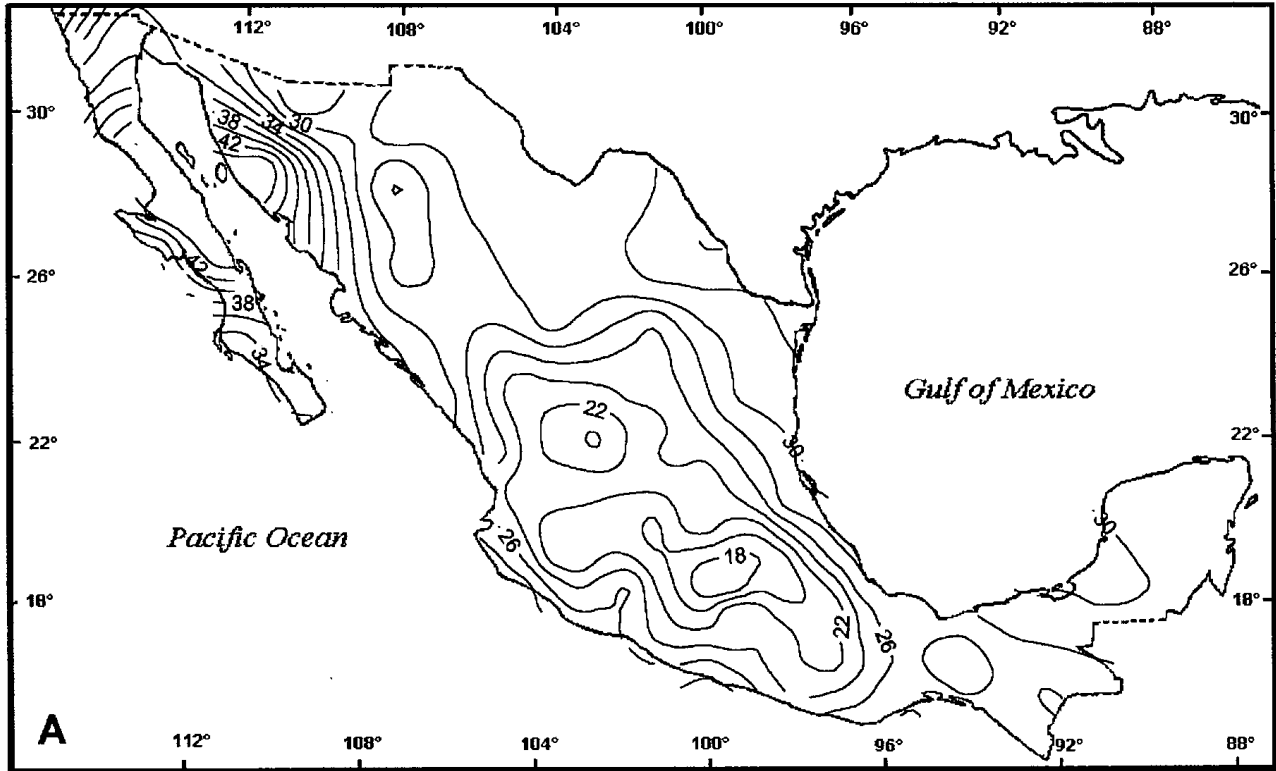


Fig. 8. Similar to Figure 7 but for July.

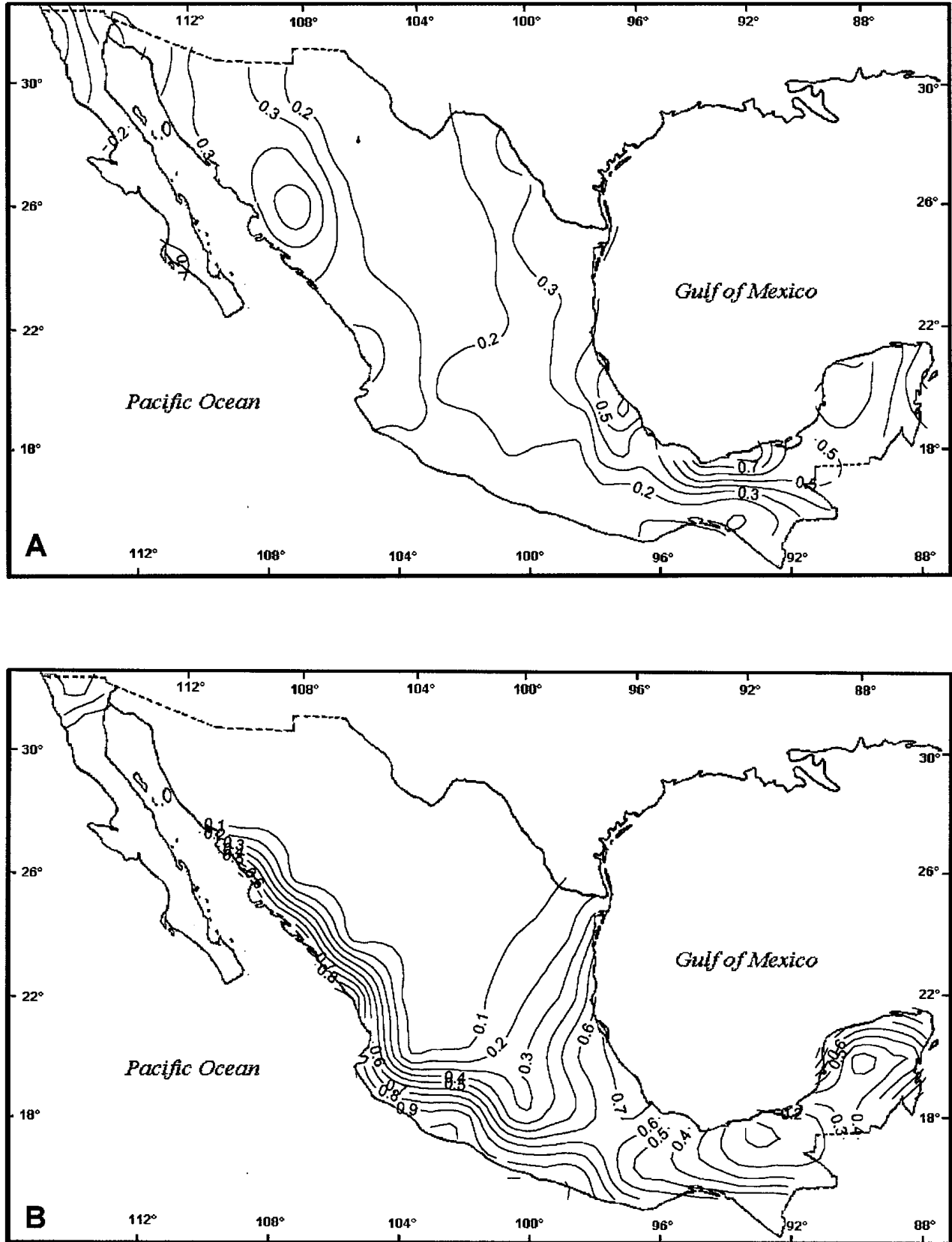


Fig. 9. Soil moisture availability for January, simulated by the model (Part A) and the quotient of the latent heat over the potential evapotranspiration, both obtained from large-scale NCEP reanalysis (Part B).

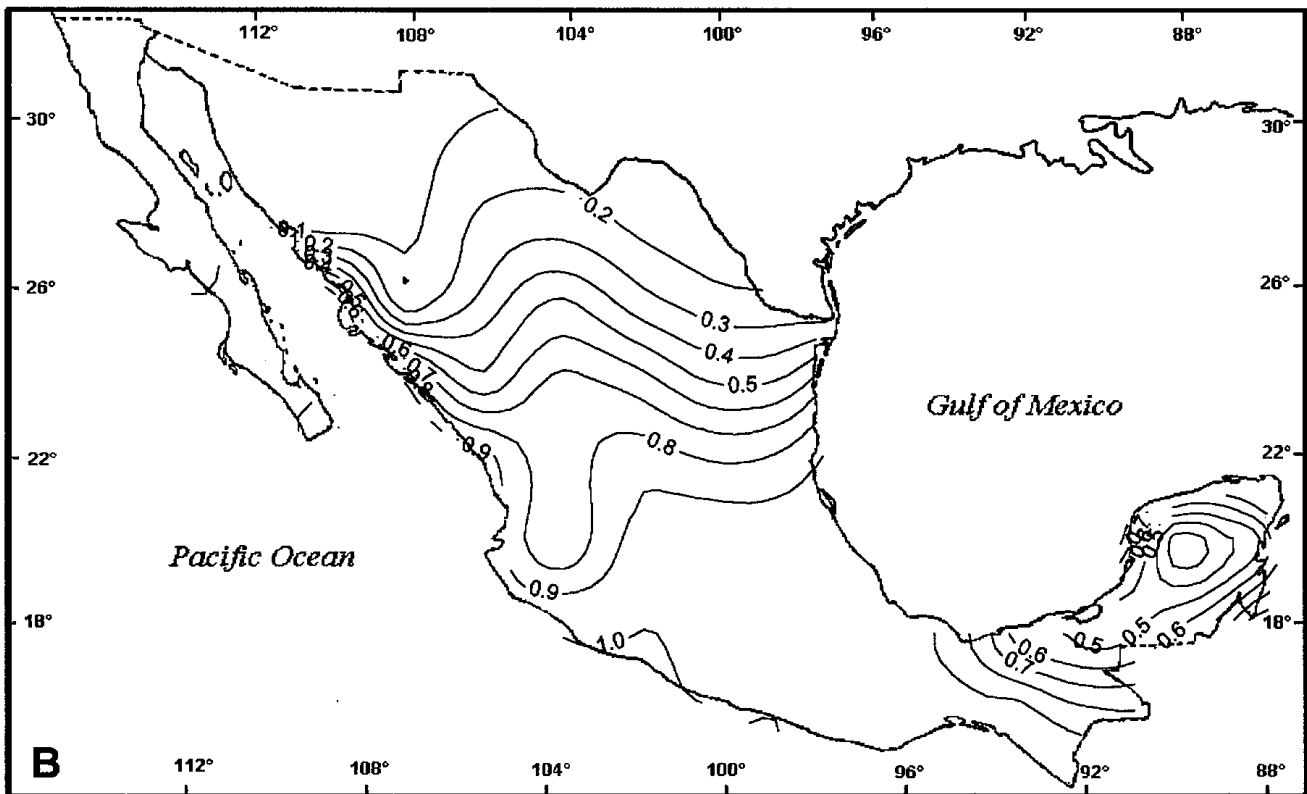
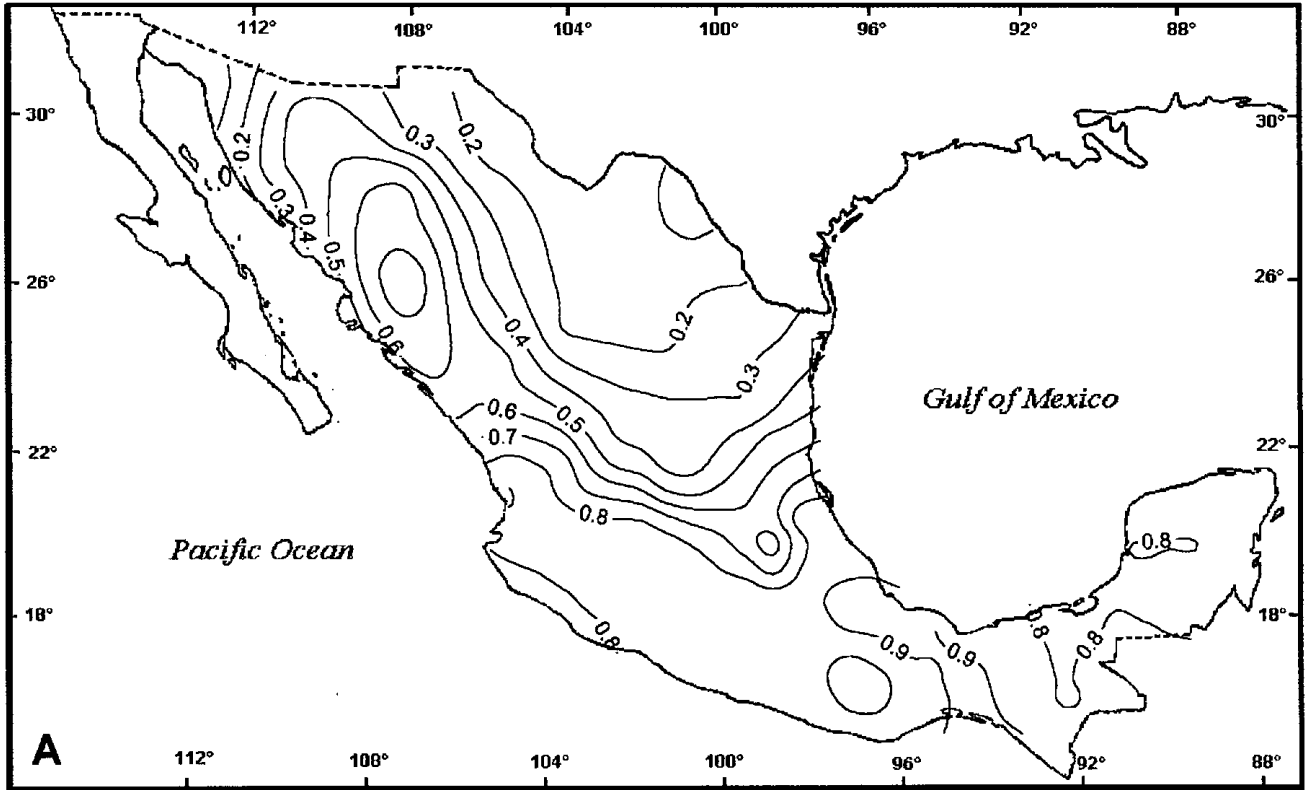


Fig. 10. Similar to Figure 9 but for July.

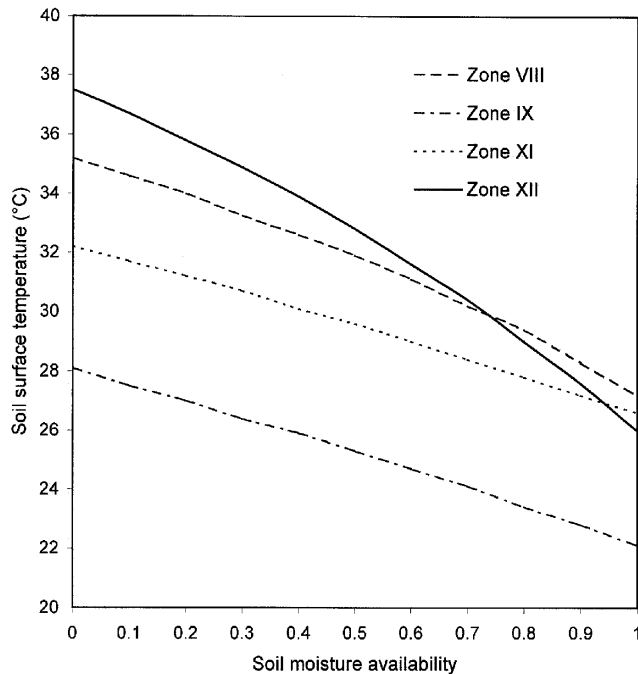


Fig. 11. Sensibility in July of the soil surface temperature, in degrees Celsius, to changes in the soil moisture availability for the 4 hydrological zones (VIII, IX, XI and XII) of northern Mexico.

tion that depends on the soil moisture availability. Consequently, giving values of soil moisture availability, we have calculated the temperature of the soil from (17) independently of the water balance Equation (18). The results indicate that the soil surface temperature presents an important sensibility to changes in the soil moisture, as is shown in the Figure 11 for the 4 hydrological zones (VIII, IX, XI and XII) of the north of Mexico in July.

The high temperatures of more than 40 Celsius degrees in the northwest of the country, simulated by the model for July, can be explained from the results shown in the Figure 11 and of the almost null soil moisture availability in that region (Figure 10, Part A), whose vegetation is of scrubs and cactus.

4. CONCLUDING REMARKS

Instead of calibrating the five hydrological parameters basin by basin, we have assigned, in base to a previous paper, constant values for all the country to four of the five parameters. The remaining parameter have been adjusted so that the annual runoff simulated by the model for all the country agree well enough with the observed annual runoff, whose value is of 208.3 mm.

The distribution and magnitude of the simulated annual flow agrees quite well with the observed one. In the

evaluation by basin, nine of the twelve hydrological zones have an error of less than 50% in the simulated annual flow and the twelve zones have an error of less than 20% in the simulation of the annual evaporation.

A future project is the construction of a thermal and hydrological balance Atlas for the Mexican Republic using this model with a higher spatial resolution to reduce the error in runoff and evaporation.

On the other hand the model also can be applied to the hydrological study of a particular basin. We have in view to apply this model to three of the basins more populous of the country: Balsas River Basin (zone IV), Pánuco River Basin (zone V) and Lerma-Chapala-Santiago Basin (zone VII).

Assuming that the hydrological parameters of the model are not modified under a global climate change, we have estimated with the first version of this model the vulnerability in the availability of water in the basins and watersheds in Mexico due to such climate change. The same study will be carry out with a new version of the model and with a greater spatial resolution.

ACKNOWLEDGMENTS

The authors are indebted to Alejandro Aguilar Sierra and Berta Oda Noda for their assistance in the development of the computer program required for displaying the figures.

BIBLIOGRAPHY

- ADEM, J., 1964. On the physical basis for the numerical prediction of monthly and seasonal temperatures in the troposphere-ocean-continent system. *Monthly Weather Review*, 92, 91-104.
- ATLAS DEL AGUA DE LA REPÚBLICA MEXICANA, 1976. Secretaría de Recursos Hidráulicos, México, 125 pp.
- BÂ, K. M., C. DÍAZ, J. LLAMAS and H. LLANOS, 1995. Zonas semiáridas y su modelación hidrológica (lluvia-escurrimiento). *Ingeniería Hidráulica en México*, X, 2, 21-31.
- BARRADAS, V. L., 1990. El efecto de la vegetación en la predicción del clima, con especial énfasis en la República Mexicana. Tesis de Maestría. Facultad de Ciencias. UNAM. 78 pp.

- BUDYKO, M. I., 1974. Climate and life. International Geophysics Series, 18, Academic Press, New York, 508 pp.
- BENJAMIN, S. G. and T. N. CARLSON, 1986. Some effects of surface heating and topography on the regional severe storm environment. Part I: Three-dimensional simulations. *Monthly Weather Review*, 114, 307-329.
- CARNAHAN, B., H. A. LUTHER and J. O. WILKS, 1969. Applied numerical methods. John Wiley and Sons, Inc. 604 pp.
- FAMIGLIETTI, J. S. and E. F. WOOD, 1994. Multiscale modelling of spatially variable water and energy balance processes. *Water Resources Research*, 30, 11, 3061-3068.
- FOGEL, M. M., L. H. HEKMAN and L. DUCKSTEIN, 1980. Predicting sediment yield from strip-mined lands. Symposium on watershed management, Boise, Idaho. Journal of irrigation and drainage Div. American Soc. of Civil Eng., 176-187.
- JAÚREGUI, E., 1978. Una primera estimación de la distribución de la radiación global y neta en México. *Recursos Hidráulicos*, VII, 2, 96-106.
- MANABE, S., 1969. Climate and ocean circulation, I. The atmospheric circulation and the hydrology of the earth's surface. *Mon. Weather Rev.*, 97, 739-774.
- MENDOZA, V. M., E. E. VILLANUEVA and J. ADEM, 1997. Vulnerability of basins and watersheds in Mexico to global climate change. *Climate Research*, 9, 139-145.
- OHTA, S., Z. UCHIJIMA, H. SEINO and Y. OSHIMA, 1993. Probable effects of CO₂-induced climatic warming on the thermal environment of ponded shallow water. *Climatic Change*, 23, 69-90.
- OKE, T. R., 1987. Boundary layer climates. Methuen: London and New York, Second Edition, 435 pp.
- SCHAAKE, J.C., 1990. From Climate to flow. Climate Change and U.S. Water Resources. Ed. Paul E. Waggoner, John Wiley and Sons. Chap. 8, 177-206, 496 pp.
- SCHAAKE, J. C., V. I. KOREN, Q. Y. DUAN, K. MITCHELL and F. CHEN, 1996. Simple water balance model for estimating runoff at different spatial and temporal scales. *J. Geophys. Res.*, 101, D3, 7461-7475.
- SOIL CONSERVATION SERVICE (SCS), US DEPT. OF AGRICULTURE (U S D A), 1960. Estimation of direct runoff from storm rainfall. National Engineering Handbook. Sec. 4, Hydrology. Washington, 10.1-10.24.
- SPRINGER, E. P., B. J. MCGURK, R. H. HAWKINS and G. B. COLTHARP, 1980. Curve numbers from watershed data. Symposium on watershed management, Boise, Idaho. Journal of irrigation and drainage Div. American Soc. of Civil Eng., 938-950.
-
- V. M. Mendoza, E. E. Villanueva and J. Adem
Centro de Ciencias de la Atmósfera, Universidad Nacional Autónoma de México.
Circuito Exterior, Ciudad Universitaria, 04510 México, D. F. México.
e-mail: victor@atmosfera.unam.mx